First experimental results from IBM/TENN/TULANE/LLNL/LBL undulator beamline at the advanced light source

J. J. Jia and T. A. Callcott
Department of Physics, University of Tennessee, Knoxville, Tennessee 37996

J. Yurkas, A. W. Ellis, and F. J. Himpsel
IBM T. J. Watson Research Center, Yorktown Heights, New York 10598

M. G. Samant and J. Stöhr
IBM Almaden Research Center, San Jose, California 95120

D. L. Ederer
Department of Physics, Tulane University, New Orleans, Louisiana 70118

J. A. Carlisle, E. A. Hudson, and L. J. Terminello
Lawrence Livermore National Laboratory, Livermore, California 94550

D. K. Shuh and R. C. C. Perera
Lawrence Berkeley Laboratory, Berkeley, California 94720

(Presented on 18 July 1994)

The IBM/TENN/TULANE/LLNL/LBL Beamline 8.0 at the advanced light source combining a 5.0 cm, 89 period undulator with a high-throughput, high-resolution spherical grating monochromator, provides a powerful excitation source over a spectral range of 70–1200 eV for surface physics and material science research. The beamline progress and the first experimental results obtained with a fluorescence end station on graphite and titanium oxides are presented here. The dispersive features in K emission spectra of graphite excited near threshold, and found a clear relationship between them and graphite band structure are observed. The monochromator is operated at a resolving power of roughly 2000, while the spectrometer has a resolving power of 400 for these fluorescence experiments. © *1995 American Institute of Physics.*

I. INTRODUCTION

Third generation synchrotron light sources present exciting new opportunities for surface and material science research. The high brightness of such sources makes many previously difficult experiments much easier to carry out or much less time consuming, especially with the aid of insertion devices such as undulators. The IBM/TENN/TULANE/LLNL/LBL undulator beamline 8.0 at the advanced light source (ALS) was commissioned last November and has been in operation for the past eight month. A fluorescence endstation built by researchers from the University of Tennessee has been used for most early experiments. Here we report on the beamline operation and some initial experiments using soft x-ray fluorescence spectroscopy.

II. BEAMLINE AND FLUORESCENCE END STATION

Beamline 8.0 consists of a U5.0 undulator and a high-throughput spherical grating monochromator with high resolution in the sub-keV photon energy range. Figure 1 shows the schematic overview of the beamline. The U5.0 undulator has 89 poles with a period of 5.0 cm. The useful harmonics are the first, third, and fifth. The first harmonic covers an energy range of 70–250 eV. From three harmonics the undulator effectively provides intense photon flux over an energy range of 70–1200 eV with continuous adjustment of the undulator gap.

The monochromator uses spherical gratings in the grazing incidence geometry. The coherent radiation out of the undulator is focused onto the water-cooled, movable entrance slit by a water-cooled SiC vertical condensing mirror. The light then goes into the grating tank in which three water-cooled holographically ruled laminar gratings with rulings of 150, 380, and 925 line/mm are mounted. The radius of each grating is 70 m. The gratings are mounted on a horizontal linear slide parallel to each other; this makes the grating change a simple linear translation of the holder. The scanning of the monochromator is achieved by rotating the grating cradle through a sine arm with the dispersed photons focused on a movable exit slit. The optimal focusing condition can be met by moving both the entrance slit and exit slits to satisfy the Rowland Geometry. For the fluorescence end station, a horizontal refocusing mirror is employed to narrow the spot size in that direction. This spherical mirror is manufactured from silica with a gold coating. The photon flux from the monochromator is estimated to be 10^{13} photons per second focused to a 100 μm$\times$100 μm spot at a resolving power of 10 000. Greater fluxes are available at reduced resolution. Table I lists principle properties of the monochromator.

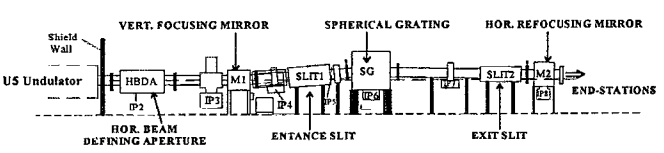

FIG. 1. The schematic overview of undulator beamline 8.0 at ALS.

 0034-6748/95/66(2)/1394/4/$6.00

TABLE I. Monochromator characteristics.

Type	Rowland circle, grazing incidence, spherical gratings
Energy range	70–1200 eV
Ver. condensing mirror	SiC, 2° grazing, water cooled, spherical
Entrance slit	Movable, water cooled
Gratings (three, 70 m radius)	150 ℓ/mm, laminar, gold coating, 70–200 eV
	380 ℓ/mm, laminar, platinum coated, 180–500 eV
	925 ℓ/mm, laminar, platinum coated, 450–1200 eV
Exit slit	Movable, uncooled
Hor. refocusing mirror	Silica, gold coated, 2° grazing, spherical
Spot size at sample	1 mm hor.×100 μm ver.
	100 μm ×100μm with hor. refocusing mirror

The soft x-ray fluorescence endstation is comprised of a Rowland circle grating emission spectrometer with a photon counting area detector and an ultrahigh vacuum (UHV) sample chamber. The sample chamber is equipped with turbomolecular, ion, and sublimation pumping. It is also fitted with a 5 keV e gun to excited fluorescence spectra when photon excitation is not critical. The system has an XYZ-θ sample manipulator which has provisions for both cryogenic and elevated temperatures, and also a sample load lock for quick sample exchange. When desired, an electron energy analyzer can be added to the sample chamber, if it is advantageous to use both photon spectroscopy and electron spectroscopy to characterize certain materials. The emission spectrometer has a fixed entrance slit rigidly mounted on a flange in the sample chamber. The grating chamber is separated from the sample chamber by a valve, where the four gratings, mounted on a carousel, are housed. The change of the gratings is accomplished by a rotary feedthrough which actuates the rotation of the carousel through spur-gears. The detector chamber is mounted on a precision X-Y-θ table, which is connected to the grating chamber by welded bellows. This design permits the detector to be scanned along either of the two Rowland Circles which are defined by the entrance slit and grating position. Both scanning and data acquisition are automated through an IEEE-488 bus interfaced to a personal computer. Figure 2 shows the outline of the endstation, while in Table II we list the major characteristics of the emission spectrometer.

III. FLUORESCENCE EXPERIMENTAL RESULTS

Soft x-ray fluorescence spectroscopy, an alternative method to photoemission to study the electronic structure of materials, has been traditionally hampered by its weak spectral intensity. However, the advent of intense monochromatic synchrotron radiation, such as that from an undulator beamline, has truly made it a viable tool to study many systems of interest. The photon-in, photon-out emission spectroscopy techniques, also have certain advantages over electron spectroscopies, because of its bulk sensitivity and its chemical and angular momentum selectivity. The tunability of the synchrotron radiation has also sparked interest in the problem of understanding of the coupling of excitation and emission processes for excitation near threshold.[1–3]

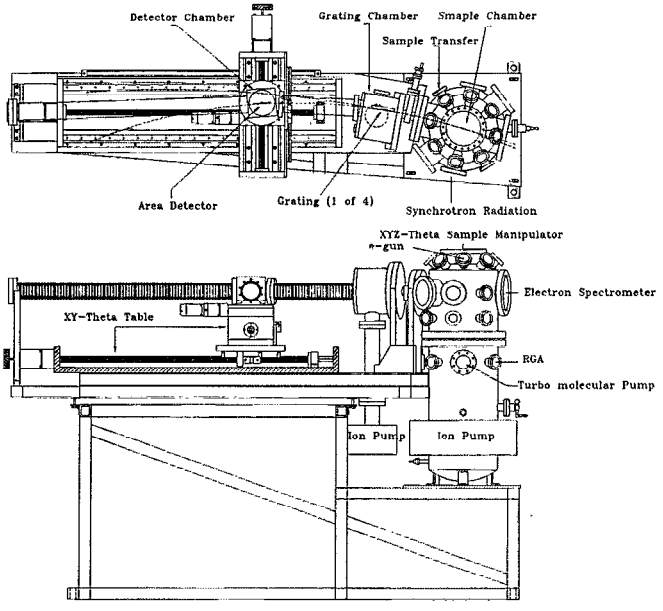

FIG. 2. The schematic sketch of the soft x-ray fluorescence endstation. The endstation consists of a 12-in. bell jar-type sample chamber and a high-efficiency emission spectrometer. The design of the spectrometer is of a grazing incidence, spherical grating, Rowland circle type.

To illustrate the capabilities of the beamline and the fluorescence endstation, we give two examples of the experiments carried out recently at the ALS.

A. Band mapping of graphite

In Fig. 3, the C-K emission spectra of highly oriented pyrolytic graphite (HOPG) excited with various photon energies, and the band structure of graphite along the high sym-

TABLE II. Spectrometer characteristics.

Type	Rowland circle, grazing incidence
Features	2–10 mm sample to slit distance
	Two angles of incidence, two Rowland circle diameters
	Four interchangeable spherical gratings
	Microchannel area detectors
Energy range	40–1000 eV
Inc. angle/Rowland dia.	2°/10 m and 4°/5 m
Gratings	5 m radius, 600 ℓ/mm, ruled gold on silica, 40–110 eV
	5 m radius, 1500 ℓ/mm, ruled gold on silica, 90–270 eV
	10 m radius, 600 ℓ/mm, ruled gold on silica, 250–680 eV
	10 m radius, 1500 ℓ/mm, etched gold on silica, 400–1000 eV
Detector	MCPs with 40 mm diameter, resistive anode
	512×512 pixels, binned to 512×16
	10%–20% quantum efficiency, 10^5 photons/s count rate
	Single photon counting
	First MCP funneled and CsI coated

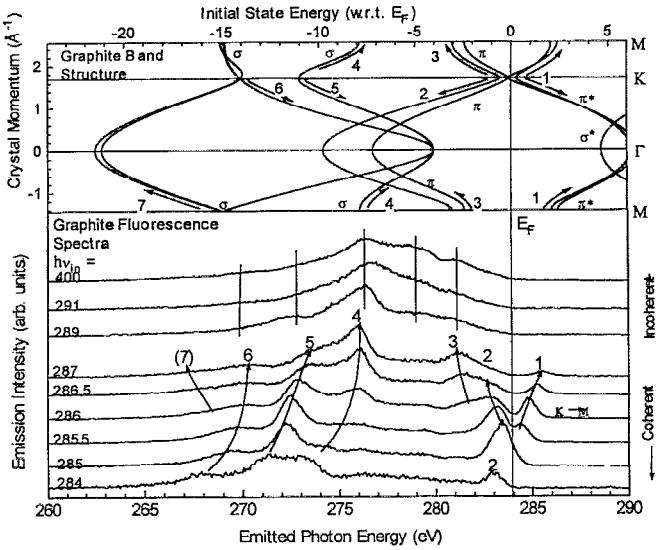

FIG. 3. The K emission spectra from HOPG graphite excited with different photon energies (lower part) and the calculated band structure of graphite (upper part).

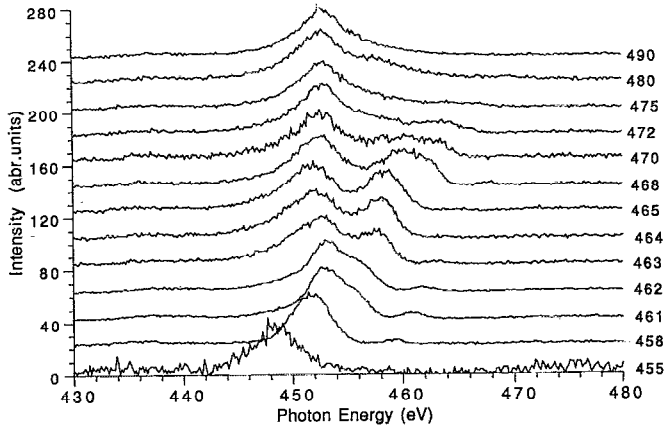

FIG. 4. The Ti $L_{2,3}$ emission spectra of TiO_2, the numbers next to the curves indicate the incident photon energies.

metry directions are shown. At an excitation energy far above threshold (400 eV), the spectrum is characteristic of the density-of-states (DOS) of graphite, with peaks originating from around critical points which are regions with higher DOS. When excitation energy is close to threshold, emission features exhibit dispersive behavior as the incident photon energy is varied, especially from 284 to 287 eV. It had been proposed recently that x-ray absorption and emission should be viewed as a single coherent inelastic scattering process when excitation is close to the core-ionization threshold.[4] Crystal momentum k is conserved in the process so that the valence electron filling the core hole has the same momentum as the core electron excited to the conduction bands. Thus band mapping of electronic states through emission spectroscopy is possible by using narrow band excitation near threshold. By varying the incident photon energy, we are exciting the core electron into unoccupied states in the conduction band with well-defined momentum. Emission occurs from filled valence states in the same region of k space, enabling one to probe the band structure of a material. The labeled bands in the lower panel of Fig. 3 arise from the occupied and unoccupied σ and π orbitals, and we can see a clear one to one correspondence between them and the σ and π bands which make up graphite band structure. The full discussion of this work has been presented in a separate paper.[5]

B. Inelastic x-ray scattering in Ti dioxide

In Fig. 4 the Ti $L_{2,3}$ emission spectra of TiO_2 are shown. As incident photon energy is tuned from 455 to 490 eV, very dramatic spectral change occurred. At high excitation energy, 490 eV, the spectrum very much resembles that obtained by e-beam excitation, and the L_2 emission is suppressed due to Coster–Kronig decay of the $2p_{1/2}$ core holes. At lower excitation energy, both elastic and inelastic features are observed. The inelastic features show a fixed energy difference from the exciting radiation and thus exhibit both resonant and dispersive behavior as the photon energy is varied. This phenomenon has been predicted and observed in K shell electrons of rare gas by Aberg and Tulkki.[6] The change in the spectra of TiO_2 is different from that of TiO or TiN, in these compounds, our spectra on TiO and those from Rubensson *et al.* on TiN[7] showed only one nondispersive resonant peak a few eV above the emission band. This resonant behavior is attributed to the localized nature of excited states where excited electrons coupled to the $2p_{1/2}$ core hole would produce a localized intermediate state which is quickly depopulated into a quasiatomic state involving the $2p_{3/2}$ core hole via a Coster–Kronig process. The subsequent radiative recombination of the intermediate states give the resonance seen in these compounds. The interpretation of TiO_2 fluorescence spectra could be useful to the general understanding of light $3d$ transition metal oxides which have been extensively studied by other spectroscopic methods such as photoemission and photoabsorption. A rigorous analysis is being carried on these spectra at the moment.

The above experimental examples clearly show the advantages of the undulator-based beamlines in third generation synchrotron sources. The band mapping is only possible with a high-resolution monochromator which delivers sufficient photon flux. The low fluorescence yield of transition metals had made it very time consuming, using a regular bend magnet beamline to obtain emission spectra from these metals and their compounds. The relative ease of getting these spectra on our undulator beamline indicates that many other experiments will benefit from the high brightness of ALS and other comparable third generation light sources.

This research was supported by National Science Foundation Grant No. DMR-9017996 through the University of Tennessee, Knoxville, and by the Division of Materials Science, Office of Basic Energy Science under the auspices of the U. S. Department of Energy by Lawrence Livermore National Laboratory under Contract No. W-7405-ENG-48. The Advanced Light Source is supported by the Office of Basic Energy Science of the Department of Energy under Contract No. DE-AC03-76SF00098.

[1] T. A. Callcott, C. H. Zhang, D. L. Ederer, D. R. Mueller, J. E. Rubensson, and E. T. Arakawa, Nucl. Instrum. Methods A **291**, 13 (1990).
[2] R. C. C. Perera, Nucl. Instrum. Methods A **319**, 277 (1992).
[3] J. Nordgren, G. Bray, S. Cramm, R. Nyholm, J.-E. Rubensson, and N. Wassdahl, Rev. Sci. Instrum. **60**, 1690 (1989).
[4] Y. Ma, N. Wassadahl, P. Skytt, J. Guo, J. Nordgren, P. D. Johnson, J. E. Rubensson, T. Boske, W. Eberharht, and S. D. Kevan, Phys. Rev. Lett. **69**, 2598 (1993).
[5] J. A. Carlisle, E. L. Shirley, E. A. Hudson, L. J. Terminello, T. A. Callcott, D. L. Ederer, R. C. C. Perera, and F. J. Himpsel (unpublished).
[6] T. Aberg and J. Tulkii, *Atomic Inner Shell Physics*, edited by Bernd Crasemann (Plenum, New York 1985).
[7] J. E. Rubensson, N. Wassadahl, G. Bray, J. Rindstedt, R. Nyholm, S. Cramm, N. Martensson, and J. Nordgren, Phys. Rev. Lett. **60**, 1759 (1988).